AGU PUBLICATIONS

JGR

Journal of Geophysical Research: Atmospheres

RESEARCH ARTICLE
10.1002/2014JD022030

Key Points:
- The major components of soluble particles are $CaSO_4$, Na_2SO_4, and NaCl
- Sulfate salt flux correlates inversely with Antarctic air temperature
- NaCl particles exist in early Holocene ice

Correspondence to:
I. Oyabu,
oyabu@lowtem.hokudai.ac.jp

Citation:
Oyabu, I., Y. Iizuka, R. Uemura, T. Miyake, M. Hirabayashi, H. Motoyama, T. Sakurai, T. Suzuki, and T. Hondoh (2014), Chemical compositions of sulfate and chloride salts over the last termination reconstructed from the Dome Fuji ice core, inland Antarctica, *J. Geophys. Res. Atmos.*, *119*, 14,045–14,058, doi:10.1002/2014JD022030.

Received 15 MAY 2014
Accepted 26 OCT 2014
Accepted article online 29 OCT 2014
Published online 16 DEC 2014

Chemical compositions of sulfate and chloride salts over the last termination reconstructed from the Dome Fuji ice core, inland Antarctica

Ikumi Oyabu[1,2], Yoshinori Iizuka[2], Ryu Uemura[3], Takayuki Miyake[4], Motohiro Hirabayashi[4], Hideaki Motoyama[4], Toshimitsu Sakurai[2,4,5], Toshitaka Suzuki[6], and Takeo Hondoh[2]

[1]Graduate School of Environmental Science, Hokkaido University, Sapporo, Japan, [2]Institute of Low Temperature Science, Hokkaido University, Sapporo, Japan, [3]Department of Chemistry, Biology and Marine Science, Faculty of Science, University of the Ryukyus, Okinawa, Japan, [4]National Institute of Polar Research, Tokyo, Japan, [5]Institute for Laser Technology, Osaka, Japan, [6]Department of Earth and Environmental Sciences, Faculty of Science, Yamagata University, Yamagata, Japan

Abstract The flux and chemical composition of aerosols impact the climate. Antarctic ice cores preserve the record of past atmospheric aerosols, providing useful information about past atmospheric environments. However, few studies have directly measured the chemical composition of aerosol particles preserved in ice cores. Here we present the chemical compositions of sulfate and chloride salts from aerosol particles in the Dome Fuji ice core. The analysis method involves ice sublimation, and the period covers the last termination, 25.0–11.0 thousand years before present (kyr B.P.), with a 350 year resolution. The major components of the soluble particles are $CaSO_4$, Na_2SO_4, and NaCl. The dominant sulfate salt changes at 16.8 kyr B.P. from $CaSO_4$, a glacial type, to Na_2SO_4, an interglacial type. The sulfate salt flux ($CaSO_4$ plus Na_2SO_4) inversely correlates with $\delta^{18}O$ in Dome Fuji over millennial timescales. This correlation is consistent with the idea that sulfate salt aerosols contributed to the last deglacial warming of inland Antarctica by reducing the aerosol indirect effect. Between 16.3 and 11.0 kyr B.P., the presence of NaCl suggests that winter atmospheric aerosols are preserved. A high $NaCl/Na_2SO_4$ fraction between 12.3 and 11.0 kyr B.P. indicates that the contribution from the transport of winter atmospheric aerosols increased during this period.

1. Introduction

The concentrations of impurities in an Antarctic deep ice core can be used as climate proxies to reconstruct the history of aerosols over the past several hundred thousand years [e.g., *Watanabe et al*., 2003a; *EPICA Community Members*, 2004, 2006]. In Antarctic ice cores, insoluble aerosols mainly contain silicates, whereas soluble aerosols contain Na^+, Mg^{2+}, Ca^{2+}, K^+, NH_4^+, H^+, SO_4^{2-}, NO_3^-, Cl^-, and methanesulfonic acid. Such proxies have revealed past climate variability on various timescales at high southern latitudes, including environmental changes in the southern parts of South America and the Southern Ocean [e.g., *Fujii et al*., 2003; *Wolff et al*., 2006, 2010; *Kaiser and Lamy*, 2010]. Primary aerosol particles are emitted directly from land and/or the sea surface, whereas secondary aerosols such as sulfate and nitrate compounds are produced by chemical reactions in the atmosphere. For example, $CaSO_4$ can be a primary aerosol, generated by terrestrial gypsum ($CaSO_4 \cdot 2H_2O$), and also a secondary aerosol, generated by neutralization of calcium carbonate ($CaCO_3$) by H_2SO_4 in the atmosphere [*Legrand et al*., 1997]. Na_2SO_4, a secondary aerosol, mainly comes from oceanic NaCl reacting with H_2SO_4 in the atmosphere [*Legrand and Delmas*, 1988; *Iizuka et al*., 2012a]. Clarifying the abundance of such primary and secondary aerosols is important for understanding past atmospheric environments.

Sulfate aerosols are a key component of cloud condensation nuclei (CCN) in the atmosphere [*Intergovernmental Panel on Climate Change (IPCC)*, 2007, 2013]. According to Köhler theory [*Köhler*, 1936], a larger aerosol particle has a lower critical supersaturation for CCN activation, which makes it more likely to become CCN. Hygroscopicity will also affect CCN activation. However, in comparing H_2SO_4 to sulfate salt, the effect from the difference in hygroscopicity is negligibly small compared to the typical differences in particle size [*Petters and Kreidenweis*, 2007]. That is, the sulfate salt, being mainly secondary aerosols of dust and sea salt [*Legrand et al*., 1997; *Legrand and Delmas*, 1988], have diameters typically exceeding 1 μm, much larger than the submicron diameters of H_2SO_4 droplets [e.g., *Whitby*, 1978]. Moreover, *Jasper et al*. [2011] argued

that H_2SO_4 is too small to be CCN, so other chemical species are needed for particle growth. Thus, CCNs are most likely more dominated by sulfate salts than by H_2SO_4.

Several studies have deduced the salt compositions from the measured ion concentrations [*Legrand et al*., 1988; *Iizuka et al*., 2008]. For Vostok ice, *Legrand et al*. [1988] calculated the sea-salt and terrestrial-salt concentrations by using seawater composition. They argued that the Holocene soluble impurities were mainly H_2SO_4, HNO_3, HCl, NaCl, and Na_2SO_4. For the Last Glacial Maximum (LGM), the ice instead contained primarily H_2SO_4, NaCl, and $CaSO_4$. For Dome Fuji ice, *Iizuka et al*. [2008] developed an ionic balance method for determining the chemical compounds of impurities. Following a suggestion by *Röthlisberger et al*. [2003a], a previous finding of *Iizuka et al*. [2006], and a result later published by *Sakurai et al*. [2011], they assumed that Ca^{2+} forms sulfate prior to Na^+, Na^+ forms Na_2SO_4 prior to NaCl, and Ca^{2+} forms sulfate prior to nitrate. For the LGM, they deduced that there were $CaSO_4$, Na_2SO_4, NaCl, and negligible H_2SO_4, whereas the Holocene had Na_2SO_4, H_2SO_4, little $CaSO_4$, and negligible NaCl.

Earlier studies used micro-Raman spectroscopy to measure micron-sized single particles in ice cores. In the Dome Fuji ice core, *Ohno et al*. [2005] found soluble impurities of $CaSO_4 \cdot 2H_2O$, $MgSO_4 \cdot 11H_2O$, and $Na_2SO_4 \cdot 10H_2O$. Later, *Ohno et al*. [2006] showed that the primary soluble impurities are $CaSO_4 \cdot 2H_2O$ for the glacial maxima and $Na_2SO_4 \cdot 10H_2O$ and $MgSO_4 \cdot 11H_2O$ for warm periods. Using the same method, *Sakurai et al*. [2011] measured the Dome Fuji ice of the last termination and suggested that most of the Ca^{2+} exists as $CaSO_4 \cdot 2H_2O$ and that the sulfate salt compositions from LGM to Holocene can be explained by ion balance arguments.

Iizuka et al. [2009] developed the sublimation-EDS (energy dispersive X-ray spectroscopy) method, which allows one to measure statistically significant numbers of chemical compositions of soluble and insoluble particles in an ice core sample. Using this method, *Iizuka et al*. [2012a, 2013] showed that sea salt in Talos Dome, a peripheral dome, remains a primary aerosol as NaCl during warm periods, whereas more than 90% of the sea salt in Dome Fuji came from a secondary aerosol as Na_2SO_4. With the same method, *Iizuka et al*. [2012b] presented a time series data set of soluble salts ($CaSO_4$, Na_2SO_4, and NaCl) and the mixture of dust and sulfates over the last 300 kyr. In contrast to the nearly constant SO_4^{2-} ($CaSO_4$, Na_2SO_4, and H_2SO_4) flux (consistent with findings at Dome C [*Wolff et al*., 2010]), the sulfate salt ($CaSO_4$ and Na_2SO_4) flux inversely correlates with temperature. This correlation suggests that the glacial-to-interglacial decrease in sulfate salts reduces the aerosol indirect effect, a decrease that may contribute to the Antarctic warming.

The last glacial termination, approximately 25.0–11.0 kyr B.P., is an important period for which to investigate relations between temperature change and the chemical composition of aerosols. In this period, the chemical compositions of soluble aerosols changed drastically [*Sakurai et al*., 2011; *Iizuka et al*., 2012b] in conjunction with the climate, which showed a warming in the Dome Fuji region of approximately 8°C [*Uemura et al*., 2012]. The temperature starts increasing around 18 kyr B.P., stagnates during 16.0–14.7 kyr B.P., and then cools during 14.7–12.7 kyr B.P. at the Antarctic Cold Reversal (ACR) [*Stenni et al*., 2011]. After the ACR, the temperature rises again, reaching its highest value around 11 kyr B.P. The cause of this fluctuation has been explained by the bipolar seesaw [*Stocker and Johnsen*, 2003], in which the temperatures of the two hemispheres oscillate via a coupling involving the Atlantic Meridional Overturning Circulation and atmospheric circulation [*Anderson et al*., 2009; *Barker et al*., 2009]. Aerosols may supply clues about these temperature changes. However, the highest time resolution study of chemical compounds of soluble and insoluble particles in this period has only eight points [*Sakurai et al*., 2011], so the nature of the particles during the transition remains unclear. To clarify how the chemical compositions of these particles have changed, we analyzed the aerosol preserved in the Dome Fuji ice core with a higher time resolution.

2. Experimental Method

2.1. Ice Core Sample

The Dome Fuji ice core was drilled at one of the highest positions of the East Antarctic ice sheet (77.2°S, 39.4°E; 3810 m asl) from 1995 to 1997. The core is 2503 m long and covers the past 340 kyr [*Watanabe et al*., 2003a]. The ice core was stored in a cold room at −50°C, which is below the eutectic temperatures of all major salts. The sample depths used here are from 326.4 m (early Holocene: 11.0 kyr B.P.) to 579.8 m (LGM: 25.0 kyr B.P.). We selected 39 core sections, each section being a cuboid of $100 \times 30 \times 5\ mm^3$. The length of each cuboid sample represents 5–10 years. The average time resolution is approximately 350 years.

2.2. Single Particle Analysis by Ice Sublimation

To analyze the embedded impurities, we followed the sublimation-EDS method [*Iizuka et al.*, 2009]. Sample surfaces were decontaminated on a clean bench in the −50°C cold room using a ceramic knife. Approximately 1 g of decontaminated sample was pulverized using a clean ceramic knife and placed on a polycarbonate membrane filter with 0.45 μm diameter pores, which was set in a sublimation chamber. This sublimation chamber was set in a −50°C freezer where clean, dry air (compression air pressure of 0.55 MPa, dew point of −65°C) flowed through at a rate of 15 L min^{-1} for 100 h.

After sublimation, each filter yielded at least 200 nonvolatile particles exceeding 0.45 μm in diameter. We measured their constituent elements and diameter using a JSM-6360LV (JEOL) SEM (scanning electron microscope) and a JED2201 (JEOL) EDS (energy dispersive X-ray spectroscopy) system. To avoid electrical charging of the filter and to improve accuracy, the filter was coated with a Pt film using magnetron sputtering (MSP-10 Magnetron Sputter) before the SEM-EDS measurement. The accelerating voltage was 20 keV to allow the electron beam to penetrate micrometer-sized particles. The X-ray spectrum of each particle was measured for 45–80 s. To be counted as a nonvolatile particle, a particle had to contain at least one of Na, Mg, Si, Al, S, Cl, K, and Ca, each with an atomic ratio (%) amount at least twice that of the error (%). We also observed C, Cr, Fe, and Pt but interpreted these peaks as artifacts from the membrane filter (C), sample mount (Cr), the stainless steel of the sublimation system (Fe), and filter coating (Pt). Other elements were only rarely detected.

2.3. Chemical Compositions of Single Particles From Their Elemental Distribution

Following *Iizuka et al.* [2009, 2012a, 2012b], we classified nonvolatile particles into insoluble dust, soluble sulfate salts, and soluble chloride salts as follows. If a particle contained Si, we regarded the particle as insoluble dust (silicate); if the particle had S, we assumed that the particle contained a sulfate salt; if it had Cl, we assumed that the particle had chloride salts. More specifically, a particle containing Ca and S was assumed to have $CaSO_4$, whereas that with Na and S was assumed to have Na_2SO_4. Any other sulfate salt particle was labeled "other-S." In the same way, for chloride salts, we assumed NaCl and the other chloride salt (other Cl).

We calculated the molar mass of $CaSO_4$, Na_2SO_4, and NaCl for each sample using the spectrum ratios of each element. The calculation procedure for the molar masses followed that described in *Iizuka et al.* [2012a, 2012b]. The moles of Na, Ca, S, and Cl were calculated from the atomic ratios measured in the EDS X-ray spectrum. When a particle has Na and S, the molar mass of Na_2SO_4 is equal to the smaller mass of either Na or S. If [Na] < [S], then [Na_2SO_4] = [Na] (μeq). If [Na] > [S], then [Na_2SO_4] = [S] (μeq). The same procedure applies to [$CaSO_4$] and [NaCl]. When a particle has Na, Ca, and S, the molar ratio of Na_2SO_4 and $CaSO_4$ depends on that of Na and Ca as follows.

If [Ca] + [Na] > [S] (μeq),

$$[CaSO_4] = \frac{[Ca]}{([Ca] + [Na])} \times [S](\mu eq),$$

$$[Na_2SO_4] = \frac{[Na]}{([Ca] + [Na])} \times [S](\mu eq).$$

If [Ca] + [Na] < [S] (μeq), [$CaSO_4$] = [Ca] (μeq), and [Na_2SO_4] = [Na] (μeq). When a particle has Na, S, and Cl, the molar ratio of Na_2SO_4 and NaCl depends on that of S and Cl as follows.

If [Na] < [S] + [Cl] (μeq),

$$[Na_2SO_4] = [Na] \times \frac{[S]}{([S] + [Cl])}(\mu eq),$$

$$[NaCl] = [Na] \times \frac{[Cl]}{([S] + [Cl])}(\mu eq).$$

If instead [Na] > [S] + [Cl] (μeq), then [Na_2SO_4] = [S] (μeq) and [NaCl] = [Cl] (μeq).

Uncertainty in the molar masses was calculated as follows. We selected a particle at random. If, for example, it contained Na and S, then we repeatedly (20 times) measured its atomic ratios of Na and S. We then

calculated the ratio of the standard deviation to the average value of the 20 measurements and obtained the coefficient of variation CV_{NaS} = 0.20. For Ca and S, we obtained CV_{CaS} = 0.22, and for Na and Cl, we obtained CV_{NaCl} = 0.20. The uncertainties of the molar ratio of $Na_2SO_4/CaSO_4$ and $NaCl/Na_2SO_4$, hereafter CV_{ratio}, were obtained by error propagation. The CV_{ratio} for the molar ratio of $Na_2SO_4/CaSO_4$ was 0.30 and that of $NaCl/Na_2SO_4$ was 0.29.

For calculating the molar masses of nonvolatile particles, we regarded each particle as an ellipsoid of revolution around the particle major axis, with major and minor axes taken from the particle shadow area. The error of this assumption was obtained by picking 200 particles at random and then measuring the deviation between their actual shadow area and comparing it to the idealized ellipse shadow area. The results showed that 95% of the particles had areas that differed by less than 20%. From this result, we calculated the error in particle volume. The total uncertainty for the molar ratio of $Na_2SO_4/CaSO_4$ was 50%, whereas that for $NaCl/Na_2SO_4$ was 49%.

2.4. Ion Concentrations

The ion concentrations (Ca^{2+}, Na^+, SO_4^{2-}, Cl^-, and NO_3^-) of 122 samples from 326.4 m to 579.8 m were analyzed using ion chromatography (Dionex DX-500) at the National Institute of Polar Research. We added these samples to the existing data set of 172 samples of *Watanabe et al.* [2003b] to make 294 samples. In the SO_4^{2-} data, we identified volcanic-eruption signal spikes (n = 8) from the original SO_4^{2-} data (n = 294) using the method of *Igarashi et al.* [2011]. The mean value M and the standard deviation σ were calculated using non-sea-salt SO_4^{2-} values, yielding M =137.6 ppb and σ = 64.6 ppb. We selected eight spikes with values exceeding $M + 2\sigma$ =266.7 ppb. The $nssSO_4^{2-}$ calculation followed the method in *Bigler et al.* [2006].

Ions fluxes were derived by multiplying the ion concentration with the reconstructed annual snow accumulation. The snow accumulation rate was derived from the $\delta^{18}O$ record [*Watanabe et al.*, 2003a] of the Dome Fuji ice core, following the equation in *Parrenin et al.* [2007], and it had an uncertainty of 17% for the LGM and 5.3% for the Holocene. The average blank contribution to the SO_4^{2-} concentration equaled 1.3% from 25.0 to 16.0 kyr B.P. and 2.1% from 16.0 to 11.0 kyr B.P. For these two periods, the corresponding values were 2.8 and 7.4% for Na^+, 5 and 38% for Ca^{2+}, and 0.5 and 1.8% for Cl^-.

2.5. Salt Inclusions Deduced From Ion Concentrations

The concentrations of $CaSO_4$, Na_2SO_4, and NaCl inclusions were calculated from the Ca^{2+}, Na^+, SO_4^{2-}, Cl^-, and NO_3^- concentrations. We applied three calculation methods (Case I to III) based on previously suggested salt formation processes. The ion-deduced values from Case I to III were examined using salt data from the sublimation-EDS method.

Case I

The Na^+ forms NaCl prior to Na_2SO_4. This case produces NaCl when the Cl^-/Na^+ ratio is close to the seawater ratio (1.8 [*Whitlow et al.*, 1992]) as *Legrand et al.* [1988] and *Röthlisberger et al.* [2003a] suggested. If $Cl^-/Na^+ \geq 1.8$, then

$[NaCl] = [Na^+]$,
$[Na_2SO_4] = 0$, and
$[CaSO_4]$ equals the smaller of $[Ca^{2+}]$ and $[SO_4^{2-}]$.

If $Cl^-/Na^+ < 1.8$ and $[Ca^{2+}] > [SO_4^{2-}]$, we assume

$[NaCl] = [Cl^-]$,
$[Na_2SO_4] = 0$, and
$[CaSO_4] = [SO_4^{2-}]$.

If $Cl^-/Na^+ < 1.8$ and $[Ca^{2+}] < [SO_4^{2-}]$, then,

$[NaCl] = [Cl^-]$,
$[Na_2SO_4]$ equals the smaller of $[Na^+] - [Cl^-]$ and $[SO_4^{2-}] - [Ca^{2+}]$, and
$[CaSO_4] = [Ca^{2+}]$.

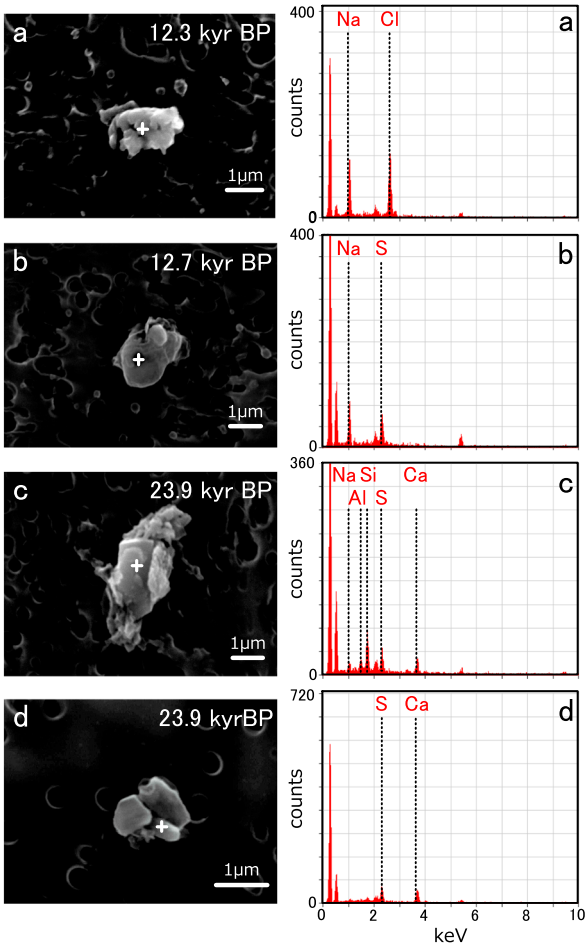

Figure 1. SEM images and X-ray spectra of particles from (a, b) warm stages and (c, d) cold stages. Representative samples are shown. NaCl from 12.3 kyr B.P. (Figure 1a), Na_2SO_4 from 12.7 kyr B.P. (Figure 1b), $CaSO_4$ and silicate mineral from 23.9 kyr B.P. (Figure 1c), and $CaSO_4$ from 23.9 kyr B.P. (Figure 1d). The left peak is C (filter), the peak second from the left is O, the peak near 2.0 keV is Pt (coating), and the peak between 5.0 and 6.0 keV is Cr (sample mount).

Case II

The Ca^{2+} forms sulfate prior to nitrate and before the Na^+ forms sulfate, whereas Na^+ forms Na_2SO_4 prior to NaCl. This case is based on ideas from papers such as *Röthlisberger et al*. [2003a], *Iizuka et al*. [2008], and *Sakurai et al*. [2011]. If $[Ca^{2+}] > [SO_4^{2-}]$, we assume the following:

$[CaSO_4] = [SO_4^{2-}]$,
$[Na_2SO_4] = 0$, and
$[NaCl] = [Na^+] + [Ca^{2+}] - [SO_4^{2-}] - [NO_3^-]$.
When this gives $[NaCl] > [Cl^-]$, we assume that $[NaCl] = [Cl^-]$, and
when this gives $[NaCl] \leq 0$, we assume that $[NaCl] = 0$.

If $[Ca^{2+}] < [SO_4^{2-}]$ and $[Ca^{2+}] + [Na^+] > [SO_4^{2-}]$, we assume that

$[CaSO_4] = [Ca^{2+}]$,
$[Na_2SO_4] = [SO_4^{2-}] - [Ca^{2+}]$, and
$[NaCl] = [Na^+] + [Ca^{2+}] - [SO_4^{2-}] - [NO_3^-]$.
Similarly, when this gives $[NaCl] > [Cl^-]$, we assume that $[NaCl] = [Cl^-]$, but
when this gives $[NaCl] \leq 0$, we assume that $[NaCl] = 0$.

If $[Ca^{2+}] + [Na^+] < [SO_4^{2-}]$, we assume that all of the Ca^{2+} and Na^+ are in the form of sulfates:

$[CaSO_4] = [Ca^{2+}]$,
$[Na_2SO_4] = [Na^+]$, and
$[NaCl] = 0$.

Case III

The Ca^{2+} forms nitrate prior to sulfate. This case is based on an implication of *Röthlisberger et al*. [2000]. If $[Ca^{2+}] > [NO_3^-] + [SO_4^{2-}]$, we assume that

$[CaSO_4] = [SO_4^{2-}]$,
$[Na_2SO_4] = 0$, and
$[NaCl]$ equals the smaller of $[Na^+]$ and $[Cl^-]$.

If $[Ca^{2+}] > [NO_3^-]$ and $[Ca^{2+}] + [Na^+] > [NO_3^-] + [SO_4^{2-}]$, we assume that

$[CaSO_4] = [Ca^{2+}] - [NO_3^-]$,
$[Na_2SO_4] = [SO_4^{2-}] + [NO_3^-] - [Ca^{2+}]$, and
$[NaCl] = [Na^+] + [Ca^{2+}] - [SO_4^{2-}] - [NO_3^-]$.
When this gives $[NaCl] > [Cl^-]$, we assume that $[NaCl] = [Cl^-]$.

If $[Ca^{2+}] > [NO_3^-]$ and $[Ca^{2+}] + [Na^+] < [NO_3^-] + [SO_4^{2-}]$, we assume that

$[CaSO_4] = [Ca^{2+}] - [NO_3^-]$,

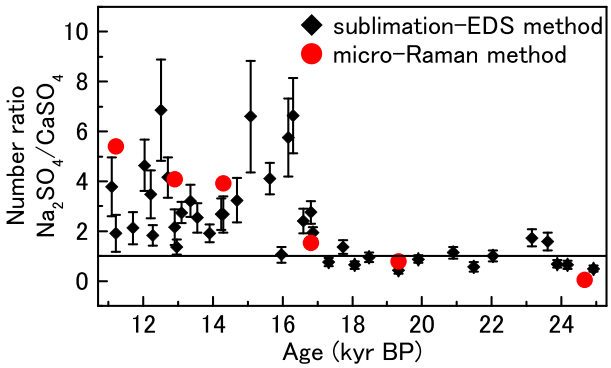

Figure 2. Number ratio of Na_2SO_4 to $CaSO_4$. Black dots indicate the ratio from the sublimation-EDS method, and red dots indicate that from the micro-Raman method [*Sakurai et al.*, 2011]. The horizontal line indicates 1. The timescale was determined by the DFO-2006 timescale [*Kawamura et al.*, 2007]. Using $\delta^{18}O$ placed on the DFGT-2003 [*Watanabe et al.*, 2003a] and DFO-2006 timescale, we set several fixed points and set up a regression line. The uncertainty is ±1.3 kyr.

$[CaSO_4] = 0$,
$[Na_2SO_4] = [SO_4^{2-}]$, and
$[NaCl] = [Na^+] + [Ca^{2+}] - [SO_4^{2-}] - [NO_3^-]$.
When this gives $[NaCl] > [Cl^-]$, we assume that $[NaCl] = [Cl^-]$.

In a later section, we propose a fourth method, Case IV.

$[Na_2SO_4] = [Na^+]$, and
$[NaCl] = 0$.

If $[Ca^{2+}] + [Na^+] < [NO_3^-]$, we assume that all of the Ca^{2+} and Na^+ are in the form of nitrate:

$[CaSO_4] = 0$,
$[Na_2SO_4] = 0$, and
$[NaCl] = 0$.

If $[Ca^{2+}] < [NO_3^-]$ and $[Ca^{2+}] + [Na^+] < [NO_3^-] + [SO_4^{2-}]$, we assume that

$[CaSO_4] = 0$,
$[Na_2SO_4] = [Na^+] + [Ca^{2+}] - [NO_3^-]$, and
$[NaCl] = 0$.

If $[Ca^{2+}] + [Na^+] > [NO_3^-]$ and $[Ca^{2+}] + [Na^+] > [NO_3^-] + [SO_4^{2-}]$, we assume that

3. Results and Discussion

3.1. Comparison of Sulfate Salt Compositions Using the Sublimation-EDS and Micro-Raman Methods

In total, we analyzed 11,262 nonvolatile particles. Figure 1 shows representative particles of the warm and cold stages. $CaSO_4$, Na_2SO_4, and NaCl are the dominant sulfate and chloride salts during the last termination in the Dome Fuji ice core, so we focused on these salts. To evaluate the abundance of sulfate salts obtained from the sublimation-EDS method, we compared the number ratio of $Na_2SO_4/CaSO_4$ obtained from the sublimation-EDS method with that of the micro-Raman method [*Sakurai et al.*, 2011]. The micro-Raman method can directly measure the sulfate composition of micron-sized salt particles in ice. Except for the data point at 24.7 kyr B.P., the number ratio of $Na_2SO_4/CaSO_4$ from the sublimation-EDS method agrees with that of the micro-Raman method (Figure 2). The sublimation-EDS method gave 0.92 ± 0.40 from 25.0 to 17.3 kyr B.P., whereas the micro-Raman method gave 0.04 at 24.7 kyr B.P. and 0.79 at 19.3 kyr B.P. The average ratio from the sublimation-EDS method after 16.8 kyr B.P. was 3.27 ± 1.76. For the micro-Raman method, the ratios at 16.8, 14.3, 12.9, and 11.2 kyr B.P. were 1.53, 3.91, 4.09, and 5.40, respectively. Thus, the sublimation-EDS method reconstructs the particle number of Na_2SO_4 and $CaSO_4$ with the same level of accuracy as the micro-Raman method.

This result suggests that chemical reactions between acids and salts are unlikely during the sublimation process. The acids (H_2SO_4, HNO_3, and HCl) should be preserved in ice cores [*Legrand et al.*, 1988; *Iizuka et al.*, 2008]. Under sublimation conditions (−50°C, 0.55 MPa), H_2SO_4 remains liquid and HNO_3 remains solid, whereas HCl becomes a volatile gas [*Ohe*, 1976; *Kulmala and Laaksonen*, 1990; *Luo et al.*, 1995; *Marion*, 2002]. However, a reaction between HCl gas and the particle is unlikely under the method's nonequilibrium conditions. Additionally, H_2SO_4 should not affect the particles during sublimation because H_2SO_4 is likely to remain on the ice crystal surfaces, away from the particles in the interior. In fact, in the ice core, H_2SO_4 collects at grain boundaries [e.g., *Fukazawa et al.*, 1998], whereas the solid particles are within grains [*Ohno et al.*, 2005]. The sublimation process takes approximately 100 h, during which time the H_2SO_4 has plenty of time to flow through the filter. We measured the filter directly at random and only detected C, O, Pt, Cr, and Fe. With no S detected on the filter, the salt compounds had little opportunity to react with H_2SO_4.

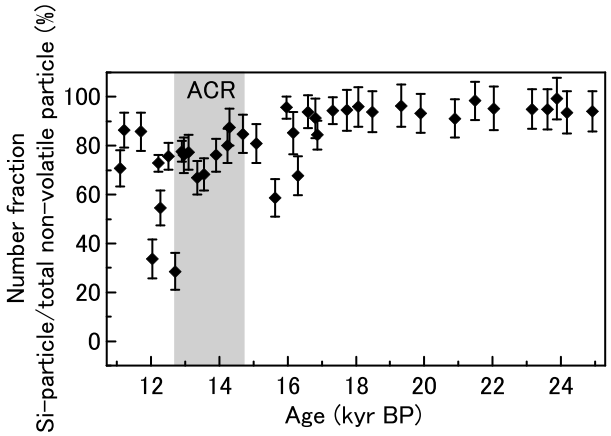

Figure 3. Number ratio of Si-containing particles to total nonvolatile particles.

3.2. Major Chemical Compositions of Nonvolatile Particles

Particles containing Si are assumed to contain silicate, a major component of insoluble particles [*Iizuka et al.*, 2009]. Most of the nonvolatile particles here contained Si. Between 25.0 and 16.6 kyr B.P., 94 ± 3% of particles contained Si (Figure 3). When the dust concentration becomes about half of the LGM level at around 16.6 kyr B.P. [*Fujii et al.*, 2003; *Röthlisberger et al.*, 2003b], the ratio starts to decrease. The ratio in 16.6–11.0 kyr B.P. showed large variability (29–96%) with an average ratio of 72 ± 16%. The significant decrease in dust concentration from the LGM increased the ratio of nonvolatile particle without Si (mainly soluble particle).

In examining 6075 sulfate and chloride particles, we found that Na_2SO_4 accounts for 42.6%, $CaSO_4$ for 20.9%, and NaCl for 23.1% of all the sulfate and chloride particles (Figure 4a). The time series of Na_2SO_4, $CaSO_4$, and NaCl particles without Si clearly showed that their fraction increases after 16.3 kyr B.P.

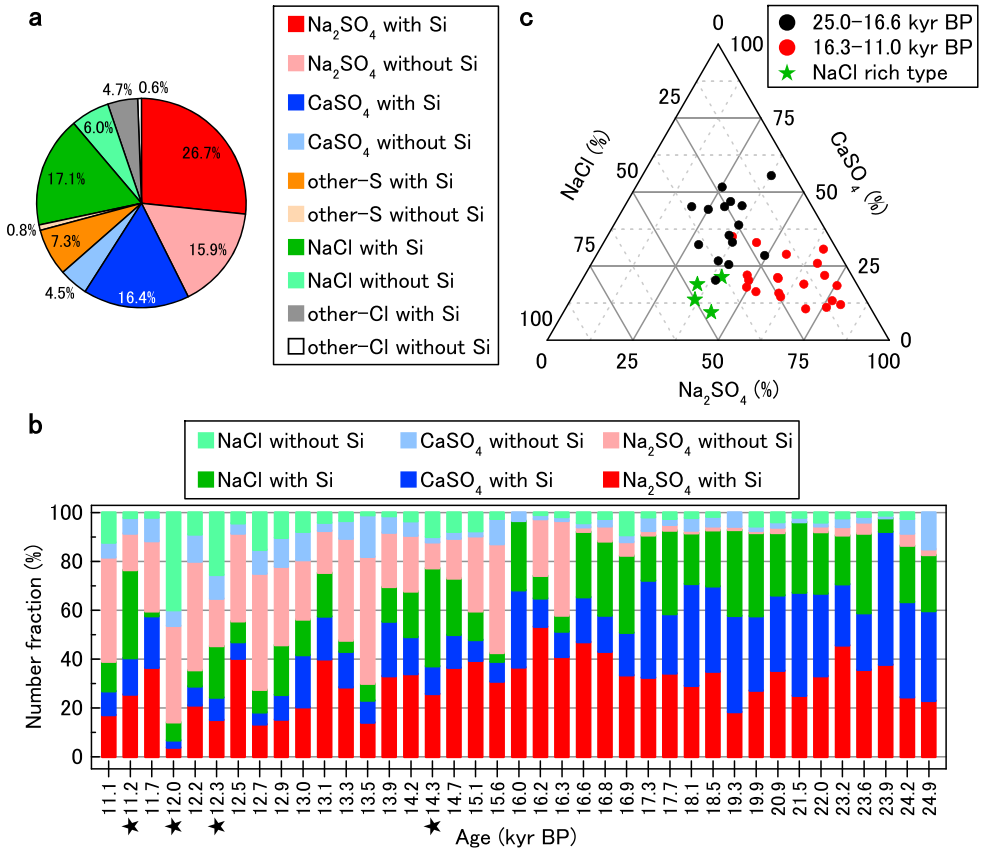

Figure 4. Chemical composition of the particles. (a) Number fraction of sulfate and chloride particles. (b) Time series number fraction of major components of sulfate and chloride salts. Age with star indicate a high NaCl fraction data point that corresponds to a "NaCl-rich type" in Figure 4c. (c) Number distribution of Na_2SO_4, $CaSO_4$, and NaCl splits into two time periods. Stars indicate irregular points of warm type (NaCl rich).

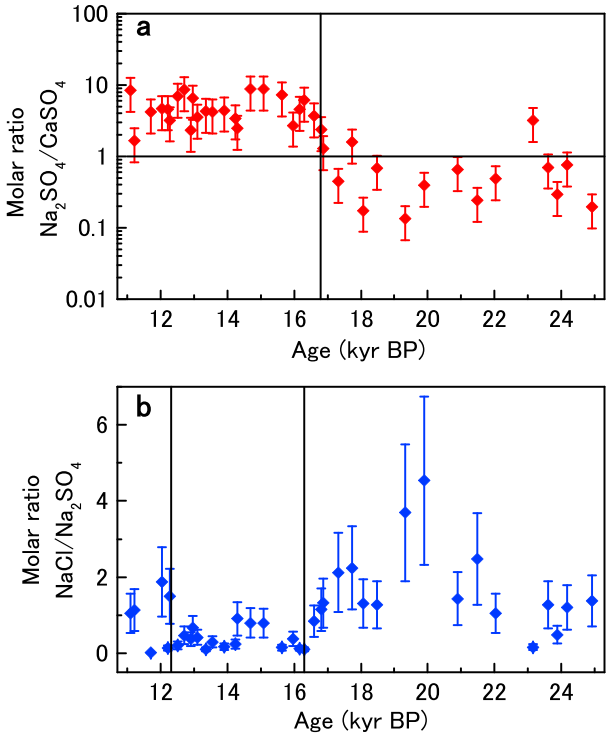

Figure 5. Molar ratios of the salt components from the sublimation-EDS method. (a) Na_2SO_4 to $CaSO_4$. The horizontal line indicates 1, and vertical line marks 16.8 kyr B.P. (b) NaCl to Na_2SO_4. The vertical lines mark 16.3 and 12.3 kyr B.P.

(Figure 4b). This change occurs when the number ratio of Si-containing particles decreases (Figure 3). Between 25.0 and 16.6 kyr B.P., 91 ± 4% of the three salts included Si. Between 16.3 and 11.0 kyr B.P., that fraction decreased to 56 ± 20%. When considering the salt type, the non-Si salt with the largest fraction was Na_2SO_4. These trends indicate that the opportunity for atmospheric aerosols such as sea salt to encounter dust decreases as the amount of dust decreases.

The salt distribution can be divided into two time periods: 25.0–16.6 kyr B.P. and 16.3–11.0 kyr B.P. (Figure 4c). For 25.0–16.6 kyr B.P., most particles have 20–55% $CaSO_4$, 20–40% Na_2SO_4, and 20–40% NaCl. That is, the fractions during this period are all approximately one third ($CaSO_4$ is 36 ± 12, Na_2SO_4 is 35 ± 9, and NaCl is 28 ± 8%). However, for 16.3–11.0 kyr B.P., the particles have 10–30% $CaSO_4$, 45–80% Na_2SO_4, and 5–30% NaCl (with four exceptions). That is, compared to the older period, the NaCl fraction decreases, the $CaSO_4$ fraction decreases (more than NaCl), and the Na_2SO_4 fraction shows a large increase. Most of the $CaSO_4$ and NaCl fraction lies below 30% with the Na_2SO_4 fraction above 40%. The four exceptions at 14.3, 12.3, 12.0, and 11.2 kyr B.P. have 9–21% $CaSO_4$, 35–43% Na_2SO_4, and 38–50% NaCl, that is, a lower Na_2SO_4 fraction and a higher NaCl fraction.

Figure 5a shows the molar ratio of $Na_2SO_4/CaSO_4$ calculated from the sublimation result. The ratio starts low at 0.66 ± 0.83 during 25.0–18.0 kyr B.P. (right side of plot), increases between 18.0 and 16.0 kyr B.P., and then stays high at 5.05 ± 2.35 through 11.0 kyr B.P. At 16.8 kyr B.P., the ratio changes from below 1 ($CaSO_4 > Na_2SO_4$) to above 1 ($CaSO_4 < Na_2SO_4$), showing the same trend as that found previously for the number ratio (Figure 2). This result indicates that the primary sulfate salt changes from $CaSO_4$ to Na_2SO_4 at 16.8 kyr B.P.

Figure 5b shows the analogous result for $NaCl/Na_2SO_4$. The ratio is high during the LGM, but then it decreases between 17.3 and 16.3 kyr B.P. After 16.3 kyr B.P., the ratio stays low. The average ratio decreases fivefold, from 2.77 ± 1.62 during 25.0–17.3 kyr to 0.54 ± 0.50 during 16.3–11.0 kyr B.P. Spikes occur at 12.3, 12.0, 11.2, and 11.1 kyr B.P. These spikes show $NaCl/Na_2SO_4$ to have high variability after 12.3 kyr B.P. The high $NaCl/Na_2SO_4$ variability is likely linked to an increase in the seasonal contribution of NaCl to the atmospheric aerosol in winter during this period. (The seasonal effect is discussed in the next section.)

The origin of Ca^{2+} is gypsum ($CaSO_4$) and $CaCO_3$. $CaCO_3$ is neutralized in the atmosphere by H_2SO_4 during its transport to inland Antarctica [*Anklin et al.*, 1997; *Tschumi and Stauffer*, 2000; *Kawamura et al.*, 2003]. Later, *Sakurai et al.* [2011] showed that the concentration of Ca^{2+} correlates strongly with the frequency of $CaSO_4$ and suggested that most Ca^{2+} ion forms $CaSO_4$ at every depth of the last termination. The Ca^{2+} concentration, therefore, can be regarded as the $CaSO_4$ concentration. From the $Na_2SO_4/CaSO_4$ ratio, we used the $CaSO_4$ flux (Figure 6b) to deduce the Na_2SO_4 flux (Figure 6c). As shown in Figure 6d, the total sulfate salt flux ($CaSO_4$ plus Na_2SO_4) has high values from 25 kyr B.P., equaling 6.5 ± 1.6 mg m^{-2} yr^{-1} at 18.0 kyr B.P. Then, from 18.0 to 14.7 kyr B.P., $CaSO_4$ decreases as Na_2SO_4 increases, resulting in a moderate

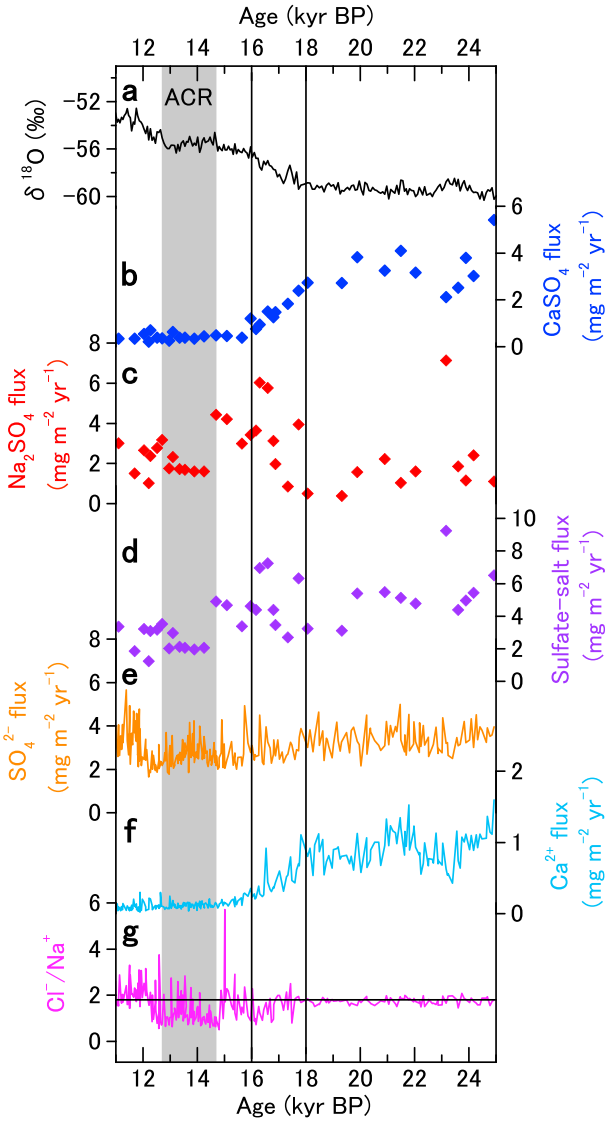

Figure 6. Time series of the fluxes. (a) $\delta^{18}O$ record from *Watanabe et al.* [2003a]. (b) $CaSO_4$ flux. (c) Na_2SO_4 flux. (d) Total sulfate salt ($CaSO_4 + Na_2SO_4$) flux. (e) SO_4^{2-} flux. (f) Ca^{2+} flux. (g) Cl^-/Na^+ record. The horizontal line is the Cl^-/Na^+ ratio in seawater (1.8) [*Whitlow et al.*, 1992]. The vertical lines mark 18.0 and 16.0 kyr B.P.

sulfate salt flux decrease. After that, the flux decreases more, reaching a low value of 2.6 ± 0.9 mg m^{-2} yr^{-1} at 11.0 kyr B.P.

As found in the last three glacial cycles [*Iizuka et al.*, 2012b], the decrease in the sulfate salt flux inversely correlates with $\delta^{18}O$ over millennial timescales (Figure 7). The squared correlation coefficient is $R^2 = 0.41$ ($p < 0.001$). This contrasts with the SO_4^{2-} flux, which showed no clear correlation with $\delta^{18}O$ (Figure 6e and 7). Sulfate salt aerosols are a key component of CCN in the atmosphere [*Köhler*, 1936; *Petters and Kreidenweis*, 2007], which lead to increased solar scattering that cools Earth's climate [*IPCC*, 2007, 2013]. The reduction in the sulfate salt flux, therefore, may have contributed to the last deglacial warming in inland Antarctica.

3.3. Validity of Ion-Deduced Sulfate and Chloride Salts

Comparisons between the sublimation-EDS method and Case I of the ion-deduced method are plotted in Figures 8a and 8b. For the $Na_2SO_4/CaSO_4$ ratio, Figure 8a shows the slope as 0.35 with a low correlation ($R^2 = 0.19$), whereas Figure 8b shows the $NaCl/Na_2SO_4$ ratio as 9.78 with a low correlation ($R^2 = 0.24$). The Case I assumption leads to too much NaCl over the entire period. The results of the micro-Raman method [*Sakurai et al.*, 2011] and the sublimation-EDS method showed that Na_2SO_4 exists not only after 16.8 kyr B.P. but before as well; however, the estimated values from Case I do not show the Na_2SO_4 between 25.0 and 16.8 kyr B.P. that was revealed in both the sublimation-EDS and the micro-Raman methods. Similar to that found at Dome C [*Röthlisberger et al.*, 2003a], the value of Cl^-/Na^+ of Dome Fuji of 16–25 kyr B.P. is close to the seawater ratio (Figure 6g). This implies that NaCl has not reacted with sulfuric acid or nitric acid. However, the data from the sublimation-EDS and the micro-Raman methods suggest that the assumption about Na^+, in which Na^+ forms NaCl when the Cl^-/Na^+ ratio is near the seawater ratio, is wrong. Here the Cl^-/Na^+ ratio is close to the seawater ratio between 25.0 and 16.8 kyr B.P., yet some Na^+ must form Na_2SO_4 instead of NaCl. The presence of Na_2SO_4 indicates the possible presence of HCl and/or other chloride salts during this period. We cannot detect HCl because HCl volatilizes during the sublimation, but we found Cl-containing particles (e.g., with $MgCl_2$). The results, therefore, suggest that the seawater Cl^-/Na^+ ratio does not necessarily indicate that NaCl has not reacted with sulfuric acid.

In contrast, Case II correlates well with the sublimation-EDS method. For the molar ratios of $Na_2SO_4/CaSO_4$, the slope is 0.96 with a high correlation ($R^2 = 0.86$) (Figure 8c). This nearly 1:1 relationship suggests that Case II deduces $CaSO_4$ and Na_2SO_4 accurately. For $NaCl/Na_2SO_4$, the slope is 0.89 with a high correlation

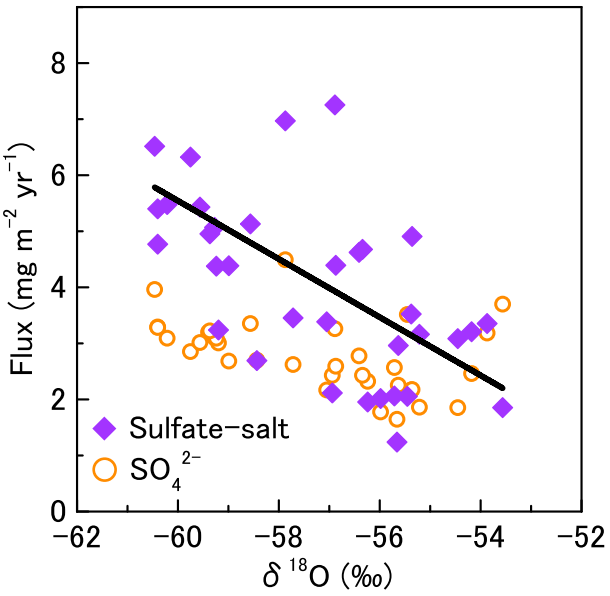

Figure 7. Correlations of sulfate salt and SO_4^{2-} fluxes to $\delta^{18}O$. The linear fitting line for sulfate salt is $F_{SALT} = -0.52\ \delta^{18}O - 25.6$ with $R^2 = 0.41$ ($n = 35$, $p < 0.001$) (Of the 39 particle samples, four had no corresponding ion measurement at the same depth).

$R^2 = 0.50$ (Figure 8d). However, Case II underestimates the [NaCl] values in 16.3–11.0 kyr B.P., giving a value of zero because $[SO_4^{2-}]$ exceeds the sum of $[Ca^{2+}]$ and $[Na^+]$. Thus, Case II poorly reconstructs NaCl during the warm period.

Case III predicts $CaSO_4$ concentrations that are too low, which makes the Na_2SO_4 concentration too high and the NaCl concentrations too low. As a result, the molar ratio of $Na_2SO_4/CaSO_4$ is too high and that of $NaCl/Na_2SO_4$ is too low. The slope for $Na_2SO_4/CaSO_4$ is 44.0 with $R^2 = 0.06$ (Figure 8e) and that for $NaCl/Na_2SO_4$ is 0.21 with $R^2 = 0.54$ (Figure 8f). Thus, Case III is not supported by the salt-inclusion data from the sublimation-EDS method.

We now propose a modification of Case II, to be called Case IV. The low values of NaCl in the warm period from Case II may be related to the seasonality of atmospheric aerosol. Aerosol observations in inland Antarctica showed that the activity of phytoplankton-producing SO_4^{2-} dominates in summer, whereas sea-salt aerosol dominates in winter [e.g., *Hara et al.*, 2004; *Preunkert et al.*, 2008; *Udisti et al.*, 2012]. A certain amount of the winter sea salt, therefore, would not encounter the summer marine biogenic sulfate and thus not fully react in the atmosphere. The 5–10 year averaging of the ion balance method would then overestimate the reaction between NaCl and SO_4^{2-}.

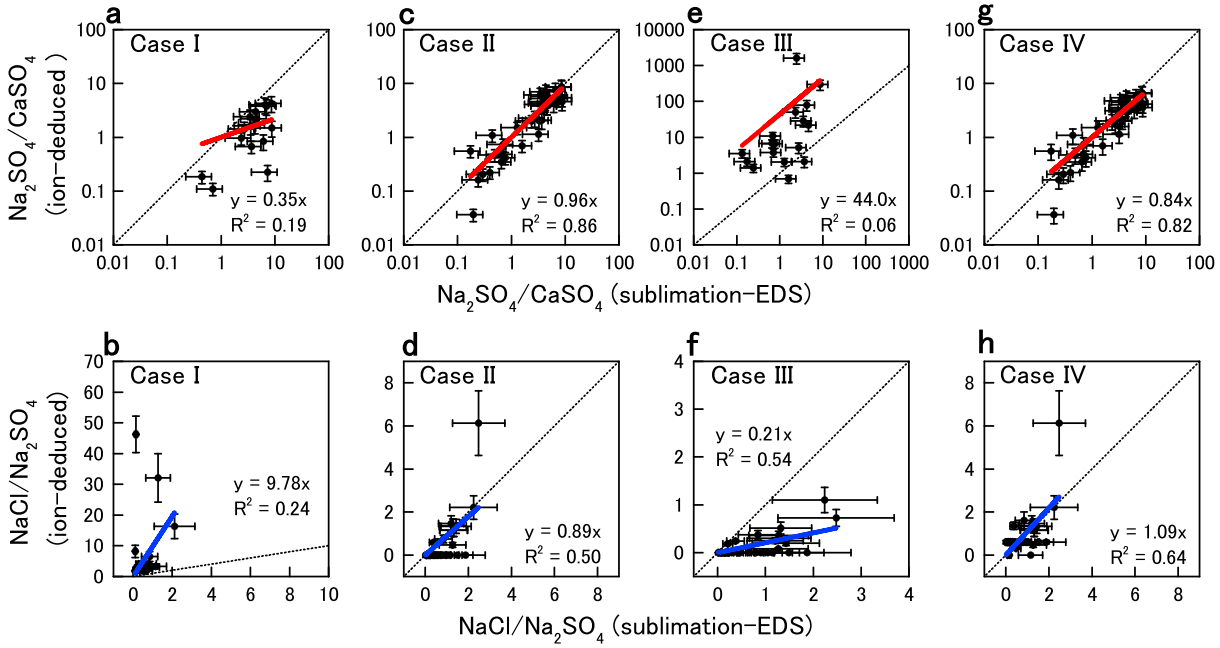

Figure 8. Comparison of ion-deduced methods to the sublimation-EDS method. (a, c, e, and g) The molar ratio $Na_2SO_4/CaSO_4$. (b, d, f, and h) $NaCl/Na_2SO_4$. Case I ion-deduced method (Figures 8a and 8b). Case II (Figures 8c and 8d). Case III (Figures 8e and 8f). Case IV (Figures 8g and 8h). The solid lines are the linear fitting lines. Dotted lines mark the 1:1 relation (Number of data points $n = 35$ for Figures 8a–8c and 8g and $n = 30$ for Figures 8d–8f and 8h. Of the 39 particle samples, four had no corresponding ion measurement at the same depth and five had an anomalous value of NO_3^-).

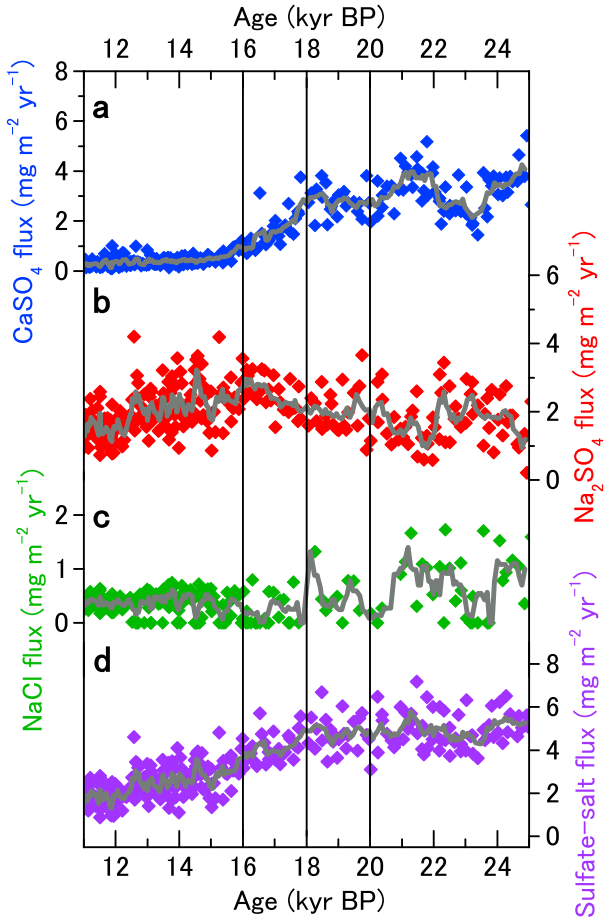

Figure 9. Time series of salt fluxes derived using the Case IV ion-deduced method. (a) $CaSO_4$ flux. (b) Na_2SO_4 flux. (c) NaCl flux. (d) Total sulfate salt ($CaSO_4 + Na_2SO_4$) flux. The vertical bars indicate 20.0, 18.0, and 16.0 kyr B.P. Solid curves are the five-point running averages.

Assuming that the chemical reaction of $2NaCl + H_2SO_4 \rightarrow Na_2SO_4 + 2HCl$ occurred completely within each single month, we calculated the monthly Na_2SO_4 and NaCl concentrations using the monthly concentrations of Na^+ and SO_4^{2-}. The Na^+ and SO_4^{2-} concentrations were measured at Dome C in 2006 [*Preunkert et al.*, 2008]. The estimated summer (December–March) concentrations are 0.17 nEq/m^3 for Na_2SO_4 and zero for NaCl. In winter (April–November), concentrations of Na_2SO_4 and NaCl are 0.24 and 0.09 nEq/m^3, respectively. The annual mean values, based on the sum of monthly estimates, are 0.22 nEq/m^3 for Na_2SO_4 and 0.07 nEq/m^3 for NaCl. Thus, by including the seasonality, we obtained a molar equivalent ratio of NaCl to Na^+ of 0.23 instead of the zero value we obtained by ignoring seasonality. We use this finding for Case IV.

Case IV

This follows Case II, except that we assume that 23% per year of Na^+ exists as NaCl in 16.3–11.0 kyr B.P.

If $[Ca^{2+}] > [SO_4^{2-}]$, then

$[CaSO_4] = [SO_4^{2-}]$,
$[Na_2SO_4] = 0$, and
$[NaCl] = [Na^+] + [Ca^{2+}] - [SO_4^{2-}] - [NO_3^-]$.
When this gives $[NaCl] > [Cl^-]$, we assume that $[NaCl] = [Cl^-]$, and when this instead gives $[NaCl] \leq 0$, then $[NaCl] = 0$.

If $[Ca^{2+}] < [SO_4^{2-}]$ and $[Ca^{2+}] + [Na^+] > [SO_4^{2-}]$, we assume that

$[CaSO_4] = [Ca^{2+}]$,
$[Na_2SO_4] = [SO_4^{2-}] - [Ca^{2+}]$, and
$[NaCl] = [Na^+] + [Ca^{2+}] - [SO_4^{2-}] - [NO_3^-]$.
When this gives $[NaCl] > [Cl^-]$, we assume that $[NaCl] = [Cl^-]$, and when this gives $[NaCl] \leq 0$, we set $[NaCl] = 0$.

If $[Ca^{2+}] + [Na^+] < [SO_4^{2-}]$ (16.3–11.0 kyr B.P.), then

$[CaSO_4] = [Ca^{2+}]$,
$[Na_2SO_4] = [Na^+] - 0.23[Na^+]$, and
$[NaCl] = 0.23[Na^+]$.

The resulting $NaCl/Na_2SO_4$ ratios from Case IV fit the sublimation-EDS method (Figure 8h) better than those from Case II. Both the slope and the R^2 value have improved. For $Na_2SO_4/CaSO_4$, the method also agrees well with the sublimation-EDS method, with a regression slope of 0.84 ± 0.07 and $R^2 = 0.82$ (Figure 8g). Thus,

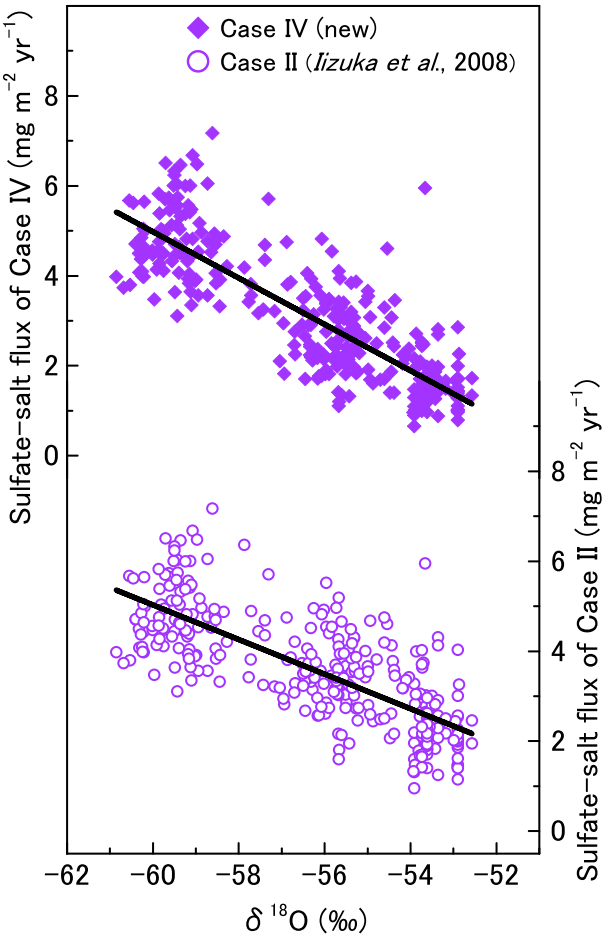

Figure 10. Total sulfate salt flux versus $\delta^{18}O$ for Cases II and IV. The linear fitting line for Case IV is $F_{SALT} = -0.51\ \delta^{18}O - 25.9$ with $R^2 = 0.71$ ($n = 286$, $p < 0.001$) and that for Case II is $F_{SALT} = -0.38\ \delta^{18}O - 18.1$ with $R^2 = 0.56$ ($n = 286$, $p < 0.001$).

the Case IV method reproduces not only $CaSO_4$ and Na_2SO_4 but also the NaCl concentration. Additionally, the agreement between Case IV and the sublimation-EDS results suggests that winter atmospheric aerosols are well preserved for at least the most recent 16 kyr.

The $CaSO_4$, Na_2SO_4, and NaCl fluxes based on Case IV are shown in Figure 9. The $CaSO_4$ flux shows the high value of $3.1 \pm 0.8\ mg\ m^{-2}\ yr^{-1}$ during 25.0–18.0 kyr B.P., but then it decreases dramatically around 18.0–16.0 kyr B.P. After that, the flux stays low at $0.4 \pm 0.2\ mg\ m^{-2}\ yr^{-1}$. In contrast, the Na_2SO_4 flux of $1.6 \pm 0.4\ mg\ m^{-2}\ yr^{-1}$ slightly increases from 20.0 kyr B.P., reaching a high value of $2.8 \pm 0.4\ mg\ m^{-2}\ yr^{-1}$ around 16.0 kyr B.P. After 16.0 kyr B.P., this flux decreases with high variability, then reaches the low value of $1.6 \pm 0.4\ mg\ m^{-2}\ yr^{-1}$ at 11.0 kyr B.P. The NaCl flux has a relatively high value with high variability ($0.7 \pm 0.6\ mg\ m^{-2}\ yr^{-1}$) until 20.0 kyr B.P. Then, this flux becomes low and stable ($0.4 \pm 0.2\ mg\ m^{-2}\ yr^{-1}$).

Consider the total sulfate salt flux ($CaSO_4$ plus Na_2SO_4), in the LGM ice, it has a value of $5.3 \pm 0.6\ mg\ m^{-2}\ yr^{-1}$ (Figure 9d) and starts to decrease around 18.0 kyr B.P. After that, the flux decreases moderately, reaching the low value of $1.8 \pm 0.4\ mg\ m^{-2}\ yr^{-1}$ at 11.0 kyr B.P. This sulfate salt flux also correlates inversely with $\delta^{18}O$ (Figure 10). The squared correlation coefficient is $R^2 = 0.71$ ($p < 0.001$), which is stronger than that from the previous ion-deduced method based on Case II ($R^2 = 0.56$, $p < 0.001$). This stronger correlation suggests that sulfate salt aerosols likely contributed to the last deglacial warming of inland Antarctica by reducing the aerosol indirect effect.

4. Conclusion

We presented the chemical compositions of nonvolatile particles during the last termination in the Dome Fuji ice core with a 350 year resolution. The results obtained using the sublimation-EDS method agreed well with the existing record obtained by Raman spectroscopy, indicating that the sublimation-EDS method for extracting nonvolatile particles does not suffer from contamination.

Using the sublimation-EDS method, the major components of the insoluble particles were found to be silicate, whereas that of the soluble particles were $CaSO_4$, Na_2SO_4, and NaCl salts. Starting with the oldest ice, the dominant sulfate salt changed at 16.8 kyr B.P. from $CaSO_4$, a glacial type, to Na_2SO_4, an interglacial type. The derived sulfate salt flux ($CaSO_4$ plus Na_2SO_4) began at the high value of $6.1 \pm 1.6\ mg\ m^{-2}\ yr^{-1}$ and then started to decrease from 18.0 kyr B.P. reaching a low value of $1.6\ mg\ m^{-2}\ yr^{-1}$ at 11.0 kyr B.P. The decrease in the sulfate salt flux correlated inversely with $\delta^{18}O$ with millennial timescales. This contrasts with the SO_4^{2-} flux, which showed no clear correlation with $\delta^{18}O$. The reduction in the sulfate salt flux likely contributed to the last deglacial warming in inland Antarctica by reducing the aerosol indirect effect.

In contrast to previous studies based on ion concentrations, the sublimation-EDS method detected NaCl in 16.3–11.0 kyr B.P. The presence of NaCl in this period suggests that winter atmospheric aerosols were preserved in the ice. In response to this finding, we proposed a new ion-deduced method by assuming that 23% per year of Na^+ exists as NaCl in Dome Fuji ice when the ionic balance satisfies $[Ca^{2+}] + [Na^+] < [SO_4^{2-}]$. The molar ratios of $NaCl/Na_2SO_4$ and $Na_2SO_4/CaSO_4$ estimated using the new ion-deduced method agreed well with that from the sublimation-EDS method. The agreement indicates that the new ion-deduced method reproduces the $CaSO_4$, Na_2SO_4, and NaCl concentrations better than previous ion-deduced methods. The sulfate salt flux from the new ion-deduced method has an inverse correlation with $\delta^{18}O$ that is stronger than that from the previous ion-deduced method. This result strongly suggests that sulfate salt aerosols contributed to the last deglacial warming of inland Antarctica by reducing the aerosol indirect effect.

Acknowledgments

We thank all members of the Dome Fuji drilling team, all participants in the Japanese Antarctic Research Expedition and Ice Core Consortium for Dome Fuji activities, S. Fujita of the National Institute of Polar Research for data revising, H. Ohno of the Kitami Institute of Technology for useful comments, M. Furusaki of the Institute of Low Temperature Science for help with EDS analysis, and J. Nelson for help with revising the manuscript. The paper was significantly improved as a result of comments by anonymous reviewers and the Scientific Editor, L. Russell, to whom we are greatly indebted. This study was supported by Young Scientists (A) (grant 23681001), Scientific Research (A) (grant 26257201), Scientific Research (S) (grant 21221002), and Challenging Exploratory Research (grant 26550013) provided by the Ministry of Education, Culture, Sports, Science and Technology (MEXT), the Japan Society for the Promotion of Science (JSPS), and by the Grant for Joint Research Program of the Institute of Low Temperature Science, Hokkaido University. Inquiries about the data used in the study can be made to the authors.

References

Anderson, R. F., S. Ali, L. I. Bradtmiller, S. H. H. Nielsen, M. Q. Fleisher, B. E. Anderson, and L. H. Burckle (2009), Wind-driven upwelling in the Southern Ocean and the deglacial rise in atmospheric CO_2, *Science*, *323*, 1443–1448, doi:10.1126/science.1167441.

Anklin, M., J. Schwander, B. Stauffer, J. Tschumi, A. Fuchs, J. M. Barnola, and D. Raynaud (1997), CO_2 record between 40 and 8 kyr B.P. from the Greenland Ice Core Project ice core, *J. Geophys. Res.*, *102*(C12), 26,539–26,545, doi:10.1029/97JC00182.

Barker, S., P. Diz, M. J. Vautravers, J. Pike, G. Knorr, I. R. Hall, and W. S. Broecker (2009), Interhemispheric Atlantic seesaw response during the last deglaciation, *Nature*, *457*, 1097–1102, doi:10.1038/nature07770.

Bigler, M., R. Röthlisberger, F. Lambert, T. F. Stocker, and D. Wagenbach (2006), Aerosol deposited in East Antarctica over the last glacial cycle: Detailed apportionment of continental and sea-salt contributions, *J. Geophys. Res.*, *111*, D08205, doi:10.1029/2005JD006469.

EPICA Community Members (2004), Eight glacial cycles from an Antarctic ice core, *Nature*, *429*, 623–628, doi:10.1038/nature02599.

EPICA Community Members (2006), One-to-one coupling of glacial climate variability in Greenland and Antarctica, *Nature*, *444*, 195–198, doi:10.1038/nature05301.

Fujii, Y., M. Kohno, S. Matoba, H. Motoyama, and O. Watanabe (2003), A 320 k-year record of microparticles in the Dome Fuji, Antarctica ice core measured by laser-light scattering, *Mem. Natl. Inst. Polar Res. Spec.*, *57*, 46–62.

Fukazawa, H., K. Sugiyama, S. Mae, H. Narita, and T. Hondoh (1998), Acid ions at triple junction of Antarctic ice observed by Raman scattering, *Geophys. Res. Lett.*, *25*(15), 2845–2848, doi:10.1029/98GL02178.

Hara, K., K. Osada, N. Kido, M. Hayashi, K. Matsunaga, Y. Iwasaka, T. Yamanouchi, G. Hashida, and T. Fukatsu (2004), Chemistry of sea-salt particles and inorganic halogen species in Antarctic regions: Compositional differences between coastal and inland stations, *J. Geophys. Res.*, *109*, D20208, doi:10.1029/2004JD00471.

Igarashi, M., Y. Nakai, Y. Motizuki, K. Takahashi, H. Motoyama, and K. Makishima (2011), Dating of the Dome Fuji shallow ice core based on a record of volcanic eruptions from AD 1260 to AD 2001, *Polar Sci.*, *5*, 411–420, doi:10.1016/j.polar.2011.08.001.

Iizuka, Y., T. Hondoh, and Y. Fujii (2006), Na_2SO_4 and $MgSO_4$ salts during the Holocene period derived by high-resolution depth analysis of a Dome Fuji ice core, *J. Glaciol.*, *52*, 176, doi:10.3189/172756506781828926.

Iizuka, Y., S. Horikawa, T. Sakurai, S. Johnson, D. Dahl-Jensen, J. P. Steffensen, and T. Hondoh (2008), A relationship between ion balance and the chemical compounds of salt inclusions found in the Greenland Ice Core Project and Dome Fuji ice cores, *J. Geophys. Res.*, *113*, D07303, doi:10.1029/2007JD009018.

Iizuka, Y., T. Miyake, M. Hirabayashi, T. Suzuki, S. Matoba, H. Motoyama, Y. Fujii, and T. Hondoh (2009), Constituent elements of insoluble and non-volatile particles during the Last Glacial Maximum exhibited in the Dome Fuji (Antarctica) ice core, *J. Glaciol.*, *55*, 552–562, doi:10.3189/002214309788816696.

Iizuka, Y., et al. (2012a), The rates of sea salt sulfatization in the atmosphere and surface snow of inland Antarctica, *J. Geophys. Res.*, *117*, D04308, doi:10.1029/2011JD016378.

Iizuka, Y., R. Uemura, H. Motoyama, T. Suzuki, T. Miyake, M. Hirabayashi, and T. Hondoh (2012b), Sulphate-climate coupling over the past 300,000 years in inland Antarctica, *Nature*, *490*, 81–84, doi:10.1038/nature11359.

Iizuka, Y., B. Delmonte, I. Oyabu, T. Karlin, V. Maggi, S. Albani, M. Fukui, T. Hondoh, and M. Hansson (2013), Sulphate and chloride aerosols during Holocene and last glacial periods preserved in the Talos Dome Ice Core, a peripheral region of Antarctica, *Tellus B*, *65*, 20197, doi:10.3402/tellusb.v65i0.20197.

Intergovernmental Panel on Climate Change (IPCC) (2007), *Climate Change 2007: The Scientific Basis. Contribution of Working Group I to the Fourth Assessment Report of the Intergovernmental Panel on Climate Change*, edited by S. Solomon et al., Cambridge Univ. Press, Cambridge, U. K., and New York.

Intergovernmental Panel on Climate Change (IPCC) (2013), *Climate Change 2013: The Physical Science Basis. Working Group I Contribution to the IPCC 5th Assessment Report—Changes to the Underlying Scientific/Technical Assessment*, edited by T. Stocker et al., Cambridge Univ. Press, Cambridge, U. K., and New York.

Jasper, K., et al. (2011), Role of sulphuric acid, ammonia and galactic cosmic rays in atmospheric aerosol nucleation, *Nature*, *476*, 429–433, doi:10.1038/nature10343.

Kaiser, J., and F. Lamy (2010), Links between Patagonian Ice Sheet fluctuations and Antarctic dust variability during the last glacial period (MIS 4-2), *Quat. Sci. Rev.*, *29*, 1464–1471, doi:10.1016/j.quascirev.2010.03.005.

Kawamura, K., T. Nakazawa, S. Aoki, S. Sugawara, Y. Fujii, and O. Watanabe (2003), Atmospheric CO_2 variations over the last three glacial–interglacial climatic cycles deduced from the Dome Fuji deep ice core, Antarctica using a wet extraction technique, *Tellus*, *55B*, 126–137, doi:10.1034/j.1600-0889.2003.00050.x.

Kawamura, K., et al. (2007), Northern Hemisphere forcing of climatic cycles in Antarctica over the past 360,000 years, *Nature*, *448*, 912–916, doi:10.1038/nature06015.

Köhler, H. (1936), The nucleus in and the growth of hygroscopic droplets, *Trans. Faraday Soc.*, *32*, 1152–1161, doi:10.1039/TF9363201152.

Kulmala, M., and A. Laaksonen (1990), Binary nucleation of water–sulfuric acid system: Comparison of classical theories with different H_2SO_4 saturation vapor pressures, *J. Chem. Phys.*, *93*, 696, doi:10.1063/1.459519.

Legrand, M. R., and R. J. Delmas (1988), Formation of HCl in the Antarctic atmosphere, *J. Geophys. Res.*, *93*, 7153–7168, doi:10.1029/JD093iD06p07153.
Legrand, M., C. Lorius, N. I. Barkov, and V. N. Petrov (1988), Vostok (Antarctica) ice core: Atmospheric chemistry changes over the last climatic cycle (160,000 years), *Atmos. Env.*, *22*(2), 317–331, doi:10.1016/0004-6981(88)90037-6.
Legrand, M., C. Hammer, M. De Angelis, J. Savarino, R. Delmas, H. Clausen, and S. J. Johnsen (1997), Sulfur-containing species (methanesulfonate and SO_4) over the last climatic cycle in the Greenland Ice Core Project (central Greenland) ice core, *J. Geophys. Res.*, *102*, 26,663–26,679, doi:10.1029/97JC01436.
Luo, B., K. S. Carslaw, T. Peter, and S. L. Clegg (1995), Vapour pressures of H_2SO_4/HNO_3/HCl/HBr/H_2O solutions to low stratospheric temperatures, *Geophys. Res. Lett.*, *22*(3), 247–250, doi:10.1029/94GL02988.
Marion, G. M. (2002), A molal-based model for strong acid chemistry at low temperatures (<200 to 298 K), *Geochim. Cosmochim. Acta*, *66*(14), 2499–2516, doi:10.1016/S0016-7037(02)00857-8.
Ohe, S. (1976), *Computer-Aided Data Book of Vapor Pressure*, Data Book Company, Tokyo.
Ohno, H., M. Igarashi, and T. Hondoh (2005), Salt inclusions in polar ice core: Location and chemical form of water-soluble impurities, *Earth Planet. Sci. Lett.*, *232*, 171–178, doi:10.1016/j.epsl.2005.01.001.
Ohno, H., M. Igarashi, and T. Hondoh (2006), Characteristics of salt inclusions in polar ice from Dome Fuji, East Antarctica, *Geophys. Res. Lett.*, *33*, L08501, doi:10.1029/2006GL025774.
Parrenin, F., et al. (2007), 1-D-ice flow modelling at EPICA Dome C and Dome Fuji, East Antarctica, *Clim. Past*, *3*, 243–259, doi:10.5194/cp-3-243-2007.
Petters, M. D., and S. M. Kreidenweis (2007), A single parameter representation of hygroscopic growth and cloud condensation nuclei activity, *Atmos. Chem. Phys.*, *7*, 1961–1971, doi:10.5194/acp-7-1961-2007.
Preunkert, S., B. Jourdain, M. Legrand, R. Udisti, S. Becagli, and O. Cerri (2008), Seasonality of sulfur species (dimethyl sulfide, sulfate, and methanesulfonate) in Antarctica: Inland versus coastal regions, *J. Geophys. Res.*, *113*, D15302, doi:10.1029/2008JD009937.
Röthlisberger, R., M. A. Hutterli, S. Sommer, E. W. Wolff, and R. Mulvaney (2000), Factors controlling nitrate in ice cores: Evidence from the Dome C deep ice core, *J. Geophys. Res.*, *105*(D16), 20,565–20,572, doi:10.1029/2000JD900264.
Röthlisberger, R., R. Mulvaney, E. W. Wolff, M. A. Hutterli, M. Bigler, M. de Angelis, and M. Hansson (2003a), Limited dechlorination of sea-salt aerosols during the last glacial period: Evidence from the European Project for Ice Coring in Antarctica (EPICA) Dome C ice core, *J. Geophys. Res.*, *108*(D16), 4526, doi:10.1029/2003JD003604.
Röthlisberger, R., R. Mulvaney, E. W. Wolff, M. A. Hutterli, M. Bigler, S. Sommer, and J. Jouzel (2003b), Dust and sea salt variability in central East Antarctica (Dome C) over the last 45 kyrs and its implications for southern high-latitude climate, *Geophys. Res. Lett.*, *29*(20), 1963, doi:10.1029/2002GL015186.
Sakurai, T., H. Ohno, S. Horikawa, Y. Iizuka, T. Uchida, K. Hirakawa, and T. Hondoh (2011), The chemical forms of water-soluble microparticles preserved in the Antarctic ice sheet during Termination I, *J. Glaciol.*, *57*(206), 1027–1032, doi:10.3189/002214311798843403.
Stenni, B., et al. (2011), Expression of the bipolar see-saw in Antarctic climate records during the last deglaciation, *Nat. Geosci.*, *4*, 46–49, doi:10.1038/ngeo1026.
Stocker, T. F., and S. J. Johnsen (2003), A minimum thermodynamic model for the bipolar seesaw, *Paleoceanography*, *18*(4), 1087, doi:10.1029/2003PA000920.
Tschumi, J., and B. Stauffer (2000), Reconstructing past atmospheric CO_2 concentration based on ice-core analyses: Open questions due to in situ production of CO_2 in the ice, *J. Glaciol.*, *46*, 152, 45–53, doi:10.3189/172756500781833359.
Udisti, R., et al. (2012), Sea spray aerosol in central Antarctica. Present atmospheric behaviour and implications for paleoclimatic reconstructions, *Atmos. Env.*, *52*, 109–120, doi:10.1016/j.atmosenv.2011.10.018.
Uemura, R., V. Masson-Delmotte, J. Jouzel, A. Landais, H. Motoyama, and B. Stenni (2012), Ranges of moisture-source temperatures estimated from Antarctic ice cores stable isotope records over glacial-interglacial cycles, *Clim. Past.*, *8*, 1109–1125, doi:10.5194/cp-8-1109-2012.
Watanabe, O., J. Jouzel, S. Johnsen, F. Parrenin, H. Shoji, and N. Yoshida (2003a), Homogeneous climate variability across East Antarctica over the past three glacial cycles, *Nature*, *422*, 509–512, doi:10.1038/nature01525.
Watanabe, O., et al. (2003b), General tendencies of stable isotopes and major chemical constituents of the Dome Fuji deep ice core, *Mem. Natl. Inst. Polar Res. Spec.*, *57*, 1–24.
Whitby, K. T. (1978), The physical characteristics of sulfur aerosols, *Atmos. Environ.*, *12*, 135–159, doi:10.1016/0004-6981(78)90196-8.
Whitlow, S., P. A. Mayewski, and J. E. Dibb (1992), A comparison of major chemical species seasonal concentration and accumulation at the South Pole and Summit, Greenland, *Atmos. Environ, Part A*, *26*, 2045–2054, doi:10.1016/0960-1686(92)90089-4.
Wolff, E. W., et al. (2006), Southern Ocean sea-ice extent, productivity and iron flux over the past eight glacial cycles, *Nature*, *440*, 491–496, doi:10.1038/nature04614.
Wolff, E. W., et al. (2010), Changes in environment over the last 800,000 years from chemical analysis of the EPICA Dome C ice core, *Quat. Sci. Rev.*, *29*, 285–295, doi:10.1016/j.quascirev.2009.06.013.